Photoluminescence properties of $Y_{0.75-x}Gd_xAl_{0.10}BO_3:Eu^{3+}_{0.10}$, $0.05R^{3+}$ (R= Sc, Bi) ($0.00 \leq x \leq 0.45$)*

Li Jie(李 杰), Wang Yu-Hua(王育华)†, Dong Qi-Zheng(董其铮), and Liu Ji-Di(刘吉地)

Department of Material Science, School of Physics Science and Technology, Lanzhou University, Lanzhou 730000*, China*

(Received 11 September 2009; revised manuscript received 14 November 2009)

$Y_{0.75-x}Gd_xAl_{0.10}BO_3:Eu^{3+}_{0.10}$, $0.05R^{3+}$ (R=Sc, Bi) ($0.00 \leq x \leq 0.45$) powder samples are prepared by solid-state reaction and their luminescence properties are investigated. With the replacement of Y^{3+} ions by Sc^{3+} (or Bi^{3+}) and Gd^{3+} ions in (Y,Al)BO_3:Eu, the intensities of emission at 254 and 147 nm are remarkably improved, because Sc^{3+} ions can absorb UV light and transfer the energy to Eu^{3+} ions efficiently. Moreover, Gd^{3+} and Bi^{3+} ions act as an intermediate "bridge" between the sensitizer and the activator (Eu^{3+}) in energy transfer to produce light in the (Y, Gd)BO_3:Bi^{3+}, Eu^{3+} system more effectively. After doping an appropriate concentration of Gd^{3+} into $Y_{0.50}Gd_{0.25}Al_{0.10}BO_3:Eu^{3+}_{0.01}$, $Bi^{3+}_{0.05}$, the emission intensity reaches its maximum, which is nearly 110% compared with the red commercial phosphor (Y,Gd)BO_3:Eu and better chromaticity coordinates (0.650, 0.350) are obtained.

Keywords: Sc^{3+}, Bi^{3+}, Gd^{3+}, luminescence intensity, chromaticity

PACC: 3320N, 3320L, 7855

1. Introduction

Tricolour inorganic luminescent materials are used in PDP to emit red, green and blue light. Both high luminescent efficiency and good colour purity are required for PDP and Hg-free lamps. Among the red phosphors, (Y, Gd)BO_3:Eu is widely used today, but its main emission peak is in the vicinity of 591 nm, leading to a poor chromaticity.[1] Recently, much research has been done to find new red phosphors,[2−5] as their luminescent efficiency is not satisfactory.

Therefore research on improving current phosphors is urgently required. Introducing other ions into the borate host may be a good method to reduce its crystal symmetry and improve the energy transfer efficiency. Better chromaticity and strong intensity were obtained when Al^{3+} ions were introduced.[6] Selecting the sensitizer for the activator is an appropriate way to improve the luminous efficiency. The absorption energy of the sensitizer can transfer directly or through other ions to the activator. For example, energy transfer from Ce^{3+} ions to Tb^{3+} ions occurs via the Gd^{3+} sublattices in $GdB_3O_6:Ce^{3+}$, and Tb^{3+} ions were investigated in Ref. [7]. The luminescent properties of (Y, Gd)BO_3:Bi^{3+}, Eu^{3+} and YBO_3:Bi^{3+}, Eu^{3+} under vacuum ultraviolet excitation (VUV) were reported recently and energy transfer from the Bi^{3+} ion to the Eu^{3+} ion was also observed.[8] The Sc^{3+} ion could absorb ultraviolet (UV) light and transfer the energy to the Eu^{3+} ion effectively to improve the photoluminescence of Eu^{3+} ion doped oxide phosphors.[9] Referring to Wang's research[6,10] and our verification experiments, the best concentrations of both Bi^{3+} ions and Sc^{3+} ions are both 5% and those of Al^{3+} and Eu^{3+} are both 10% respectively in (Y, Gd)BO_3.

However, the real role of Gd^{3+} in red phosphor (Y, Gd)BO_3:Eu is still not well understood.[11] In order to improve the luminescence efficiency and chromaticity of red phosphors further, it is necessary to study the detailed excitation process and energy transfer path under VUV excitation. In this paper, we investigate the effects of Gd^{3+} and Bi^{3+} ions on the luminescence characteristics in detail and obtain improved red phosphors.

*Project supported by the National Natural Science Foundation of China (Grant No. 10874061), the Doctoral Program Foundation of Institutions of Higher Education of China (Grant No. 20040730019), and the Project of the Combination of Industry and Research by the Ministry of Education and Guangdong Province of China (Grant No. 0712226100023).

†Corresponding author. E-mail: wyh@lzu.edu.cn

© 2010 Chinese Physical Society and IOP Publishing Ltd

2. Experiment

The $Y_{0.75-x}Gd_xAl_{0.10}BO_3$:$Eu^{3+}_{0.10}$, $0.05R^{3+}$ (R=Sc, Bi) ($0.00 \leq x \leq 0.45$) samples were synthesized from sources of Gd_2O_3 (99.99%) Y_2O_3 (99.99%), Eu_2O_3 (99.99%), Al_2O_3 (98%), Sc_2O_3 (99.99%), Bi $(NO_3)_3{\cdot}5H_2O$ (99.0%) and H_3BO_3 (98.0%). The stoichiometric values of starting materials with 20% excess of H_3BO_3 were weighed to compensate the evaporation loss at high temperature. After being ground with ethanol, the mixture was heated at 500 °C for 2.5 h, then calcined at 1100 °C for 3 h in air and cooled down to room temperature for getting the samples.

The samples obtained were characterized by a Rigaku D/max 2400 x-ray powder diffractometer (XRD) with Ni-filtered CuKα radiation. Excitation and emission spectra under ultraviolet (UV) were measured by a Xe lamp (FLS-920T with a resolution of 0.10 nm). All of the luminescence spectra in the VUV region were acquired using a deuterium lamp (V06) attached to a VUV monochromator (ARC, VM504 with a resolution of 0.06 nm) for excitation. The VUV excitation spectra were corrected through being divided by the excitation intensity of sodium salicylate under the same measurement conditions. All the above measures are recorded at room temperature.

3. Results and discussion

3.1. The x-ray diffraction analysis

All the powder samples of $Y_{0.75-x}Gd_xAl_{0.10}BO_3$:$Eu^{3+}_{0.10}$, $0.05R^{3+}$ (R=Sc, Bi) ($0.00 \leq x \leq 0.45$) exhibit white colour in body. Figure 1 displays the XRD patterns of $Y_{0.95-x}Gd_xAl_{0.10}BO_3$:$Eu^{3+}_{0.10}$, $0.05R^{3+}$ (R=Sc, Bi; x = 0.00, 0.25, 0.45). They can be recognized as single-phase systems and accord well with the literature value JCPDF card No. 16-0277, and they have no second phase observed.

The samples are indexed to a hexagonal system of vaterite type and their lattice parameters were calculated with the least-square method. For example, the unit cell parameters of $Y_{0.75-x}Gd_xAl_{0.10}BO_3$:$Eu^{3+}_{0.10}$, $Sc^{3+}_{0.05}$ ($0.00 \leq x \leq 0.45$) are shown in Fig. 2, which displays that the unit cell parameters a and c continuously increase with the increase of Gd^{3+} ion concentration. The same trends of unit parameters a and c of $Y_{0.75-x}Gd_xAl_{0.10}BO_3$:$Eu^{3+}_{0.10}$, $Bi^{3+}_{0.05}$ ($0.00 \leq x \leq 0.45$) are obtained. Because the size of the Gd^{3+} (0.94 Å, 1 Å=0.1 nm) ion is larger than that of Y^{3+} (0.89 Å),[12] Gd^{3+} ions can be successfully doped into the host and occupy lattice sites of Y^{3+} ions according to Vegard's law.

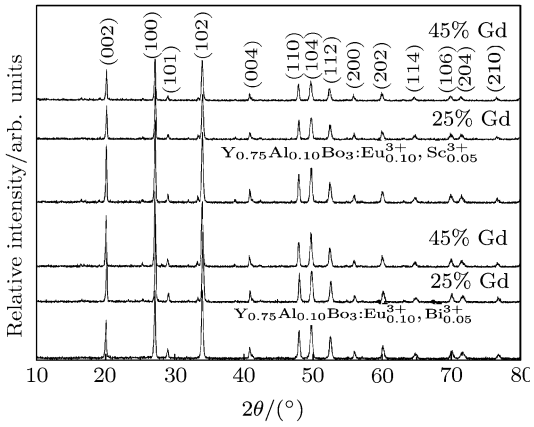


Fig. 1. XRD patterns of $Y_{0.75-x}Gd_xAl_{0.10}BO_3$: $Eu^{3+}_{0.10}$, $Sc^{3+}_{0.05}$ (Bi^{3+}) (x = 0.00, 0.25, 0.45).

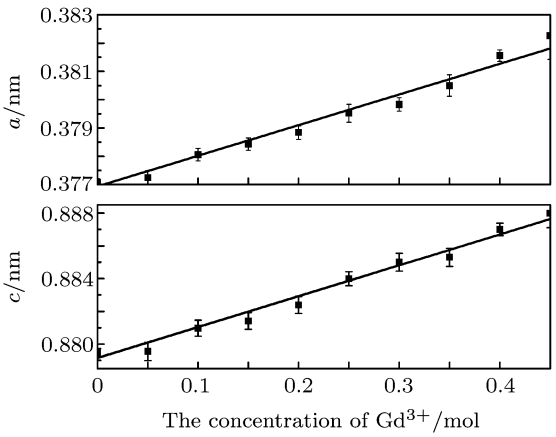


Fig. 2. Parameters a and c of the unit cell of $Y_{0.75-x}Gd_xAl_{0.10}BO_3$:$Eu^{3+}_{0.10}$, $Sc^{3+}_{0.05}$ ($0.00 \leq x \leq 0.45$).

3.2. The UV-vis spectral analysis

Figure 3 exhibits the excitation spectra of $Y_{0.75-x}Gd_xAl_{0.10}BO_3$:$Eu^{3+}_{0.10}$, $Sc^{3+}_{0.05}$ (x = 0.00, 0.10, 0.20) monitored at 612 nm. In their excitation spectra, the main broad band from 215 nm to 290 nm is assigned to the charge transfer band (CTB) of $O^{2-} \rightarrow Eu^{3+}$. After replacing some of the Y^{3+} ions with Gd^{3+} ions, the excitation intensity of the CTB is enhanced. The peak at about 275 nm could be due to the transitions of $^8S_{7/2}$ to ^6I_J (J = 11/2, 9/2, 7/2) of Gd^{3+}, which is superimposed on the CTB. This implies that an energy transfer from Gd^{3+} ions to Eu^{3+} ions could take place.[9] So the excitation intensity is enhanced with the increase of Gd^{3+} ion concentration. The peak at about 313 nm is due to the

$^8S_{7/2}$–^6P_J ($J = 11/2, 9/2, 7/2$) transition of the Gd^{3+} ion.[13] The other peaks in the wavelength region from 390 nm to 400 nm are due to the intra configuration $4f^6$ of Eu^{3+}.[14]

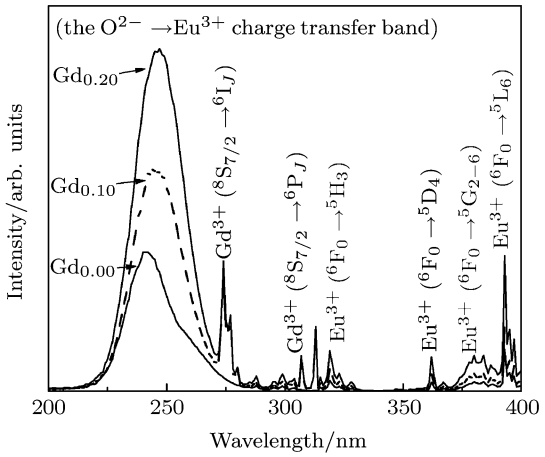


Fig. 3. Excitation spectra of luminescence of $Y_{0.75-x}Gd_xAl_{0.10}BO_3:Eu^{3+}_{0.10}$, $Sc^{3+}_{0.05}$ (x = 0.00, 0.10, 0.20) (λ_{em} = 612 nm).

The excitation spectra of $Y_{0.75-x}Gd_xAl_{0.10}BO_3$: $Eu^{3+}_{0.10}$, $Bi^{3+}_{0.05}$ (x = 0.00, 0.15, 0.25) are shown in Fig. 4. The CTB of the sample is improved when Gd^{3+} and Bi^{3+} ions are introduced into the host lattices. Compared with the CTBs of (Y, Gd)$_{0.80}Al_{0.10}BO_3:Eu^{3+}_{0.10}$ (245 nm) and $Y_{0.75-x}Gd_xAl_{0.10}BO_3:Eu^{3+}_{0.10}$, $Bi^{3+}_{0.05}$ (265 nm), the CTBs of the Bi^{3+} doping samples have a red shift of 20 nm due to the transition $^1S \rightarrow {}^3P_1$ of Bi^{3+}. The excitation peak at 265 nm is just an overlap with the CTB and due to the transitions of $^8S_{7/2}$ to ^6I_J ($J = 11/2$, 9/2, 7/2) of Gd^{3+},[8] so Gd^{3+} and Bi^{3+} ions could transfer energy adequately, i.e., an energy transfer has taken place in this case.

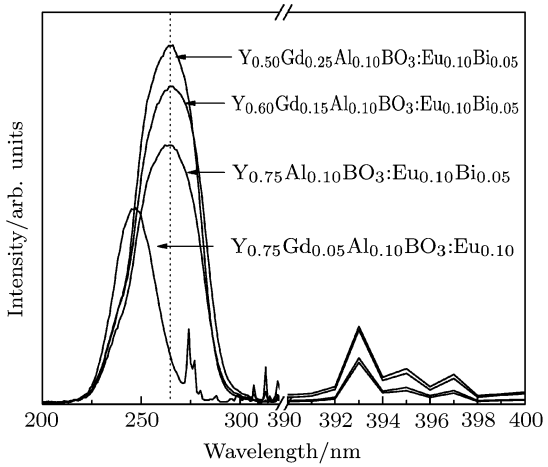


Fig. 4. Excitation spectra of the luminescence of $Y_{0.75-x}Gd_xAl_{0.10}BO_3:Eu^{3+}_{0.10}$, $Bi^{3+}_{0.05}$ (x = 0.00, 0.15, 0.25) (λ_{em} = 612 nm).

3.3. The VUV excitation spectral analysis

Figure 5 represents the excitation spectra of $Y_{0.75-x}Gd_xAl_{0.10}BO_3:Eu^{3+}_{0.10}$, $Sc^{3+}_{0.05}$ ($0.00 \leq x \leq 0.10$) under 147-nm excitation. It can be seen that the two band intensities of the synthesized samples are both much higher than that of $Y_{0.80}Al_{0.10}BO_3:Eu^{3+}_{0.10}$, indicating that VUV light can be absorbed more efficiently by borate host lattices with incorporated ions, such as Sc^{3+} and Gd^{3+}. The band around 140→160 nm is attributed to the band absorption of the host lattice,[15] which overlaps the $O^{2-} \rightarrow Gd^{3+}$ CTB.[1] The band at about 242 nm is due to the CTB of $O^{2-} \rightarrow Eu^{3+}$.[16]

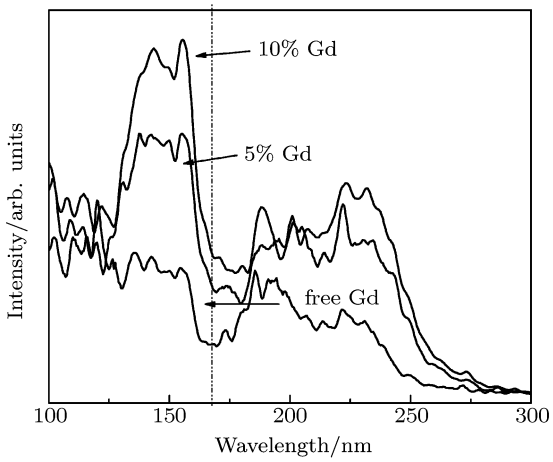


Fig. 5. Excitation spectra of $Y_{0.75-x}Gd_xAl_{0.10}BO_3:Eu^{3+}_{0.10}$, $Sc^{3+}_{0.05}$ (λ_{em} = 612 nm) ($0.00 \leq x \leq 0.10$).

3.4. The VUV emission spectral analysis

The emission spectra under 147-nm excitation are shown in Fig. 6. The shapes of all emission spectra

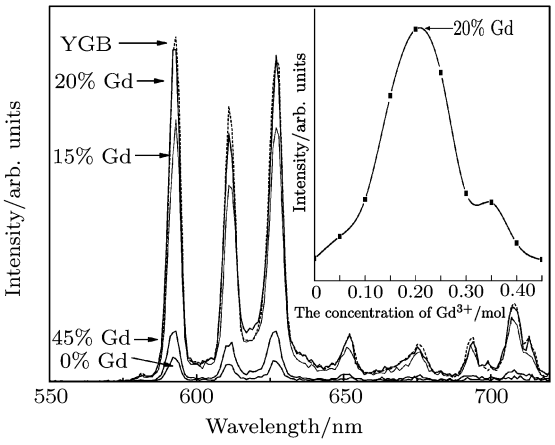


Fig. 6. Emission spectra of $Y_{0.75-x}Gd_xAl_{0.10}BO_3:Eu^{3+}_{0.10}$, $Sc^{3+}_{0.05}$ ($0.00 \leq x \leq 0.45$), with inset showing the concentration dependence of relative integrated emission intensity of these samples (λ_{ex} = 147 nm).

are similar. Typical Eu^{3+} emission is observed in these emission spectra, and the strongest emission peaks at 593 nm are due to the $^5D \rightarrow {}^7F_1$ transition of the Eu^{3+} ion. The other emission peaks located at 600 nm$\rightarrow$700 nm are ascribed to the transitions of the ^5D level to the $^7F_2$, $^7F_3$ and $^7F_4$ levels of Eu^{3+} respectively.[17] The inset in Fig. 6 exhibits that the emission intensity steadily increases with Gd^{3+} content increasing up to 0.20, and then decreases as Gd^{3+} content goes up.

Under 147-nm excitation, the integrated emission intensity of $Y_{0.55}Gd_{0.20}Al_{0.10}BO_3:Eu^{3+}_{0.10}$, $Sc^{3+}_{0.05}$ is about 99% that of the red commercial phosphor (Y, Gd)BO_3:Eu, and the chromaticity coordinates of this sample are 0.648 and 0.352, which confirms that the sample has a better colour purity than the commercial phosphor (Y, Gd)BO_3:Eu (0.632, 0.355).

Figure 7 shows a comparison between the excitation spectra of (a) $Y_{0.80}Al_{0.10}BO_3:Eu_{0.10}$, (b) $Y_{0.75}Al_{0.10}BO_3:Eu^{3+}_{0.10}$, $Bi^{3+}_{0.05}$, (c) $Y_{0.60}Gd_{0.15}Al_{0.10}BO_3:Eu^{3+}_{0.10}$, $Bi^{3+}_{0.05}$ and (d) $Y_{0.50}Gd_{0.25}Al_{0.10}BO_3:Eu^{3+}_{0.10}$, $Bi^{3+}_{0.05}$. The intensities of Eu^{3+} CTB and host absorption increase sharply with the increase of the Gd^{3+} molar fraction in samples (c) and (d). In particular, a new band from 260 nm to 280 nm is observed in samples (b), (c) and (d) separately. One band from 125 nm to 180 nm centred at about 155 nm is ascribed to the absorptions of the host and $O^{2-} \rightarrow Gd^{3+}$ CTB.[8] The other band from 180 nm to 260 nm is assigned to the CTB of $O^{2-} \rightarrow Eu^{3+}$.

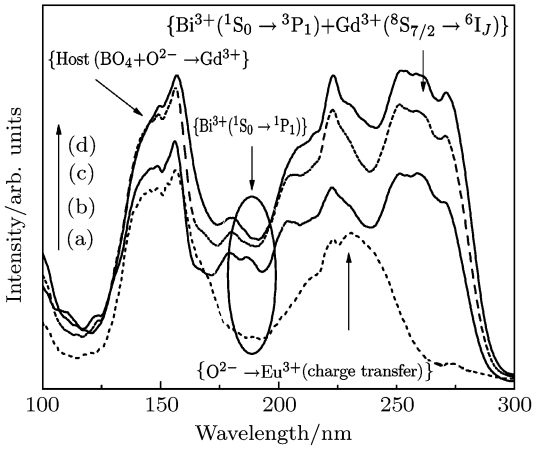


Fig. 7. Excitation spectra of (a) $Y_{0.80}Al_{0.10}BO_3$:0.01Eu, (b) $Y_{0.75}Al_{0.10}BO_3:Eu^{3+}_{0.10}$, $Bi^{3+}_{0.05}$ (c) $Y_{0.60}Gd_{0.15}Al_{0.10}BO_3:Eu^{3+}_{0.10}$, $Bi^{3+}_{0.05}$, and (d) $Y_{0.50}Gd_{0.25}Al_{0.10}BO_3:Eu^{3+}_{0.10}$, $Bi^{3+}_{0.05}$ ($\lambda_{em} = 612$ nm).

It is obvious that the two new excitation bands result from the doping of Bi^{3+} ions: one is the excitation band that is maximized at 196 nm ($^1S \rightarrow {}^1P_1$) and superimposed on the host absorption band, and the other is the band peaked at 265 nm ($^1S \rightarrow {}^3P_1$).[17] According to Ref. [8], the emission wavelength of the Bi^{3+} ion is well overlapped with the excitation band of $O^{2-} \rightarrow Eu^{3+}$, so the improvements in CTB and all the other excitation peaks can be attributed to the good sensitization effect of the Bi^{3+} ions introduced into the host lattice. This phenomenon is consistent with that of the Bi^{3+} and Eu^{3+} ion co-doped $Na_3YSi_3O_9$ host.[18]

In addition, the energy levels between $^1P_1$ of Bi^{3+} and ^6G_J of Gd^{3+}, $^3P_1$ of Bi^{3+} and ^6D_J, ^6I_J, and ^6P_J of Gd^{3+} overlap well, respectively. Therefore, the electrons in $^1P_1$ and $^3P_1$ states of Bi^{3+} can transit to ^6G_J, ^6D_J, ^6I_J, and ^6P_J levels of Gd^{3+} well through electric multipole interaction or exchange interaction, which results in Bi^{3+} transferring its absorption energy to Gd^{3+} efficiently and completely.[17,19–21] Considering the high content of Gd^{3+} ions and the low content of Bi^{3+} and Eu^{3+} ions, the energy transfer process from Bi^{3+} ions to Eu^{3+} ions probably takes place through Gd^{3+} acting as a medium, via $Bi^{3+} \rightarrow Gd^{3+} \ldots Gd^{3+} \rightarrow Eu^{3+}$. The Gd^{3+} ions act as an intermediate "bridge" between the sensitizer and the activator of Eu^{3+} in energy transfer to produce light in the (Y, Gd) $BO_3:Bi^{3+}$, Eu^{3+} system.

The energy levels in (Y, Gd)$_{0.75}Al_{0.10}BO_3:Eu^{3+}_{0.10}$, $Bi^{3+}_{0.05}$ can be calculated via its excitation spectra and they are summarized in Fig. 8. In this process, the absorption energy by host (147 nm) can be transferred to the $^1P_1$ of the Bi^{3+} ion and the CTB of $O^{2-} \rightarrow Gd^{3+}$ first. Then the excitation energy of the Gd^{3+} ion is migrated to the Gd^{3+} sublattices until it is trapped by the Eu^{3+} ion,[11,22] when the excitation energy of the Gd^{3+} ion is relaxed from levels ^6G_J, ^6D_J or ^6I_J, then transferred to level ^5D of the Eu^{3+} ion, and finally radioactively returns to levels $^7F_1$, $^7F_2$.[23]

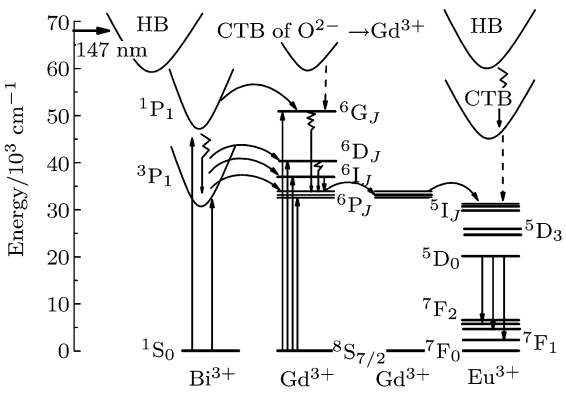


Fig. 8. Schematic diagram of energy transfer in $Y_{0.75-x}Gd_xAl_{0.10}BO_3:Eu^{3+}_{0.10}$, $Bi^{3+}_{0.05}$.

Figure 9 demonstrates the emission spectra of $Y_{0.75-x}Gd_xAl_{0.10}BO_3:Eu^{3+}_{0.10}$, $Bi^{3+}_{0.05}$ ($0.00 \leq x \leq 0.45$). The intensity continuously increases with the increase of Gd^{3+} concentration. The inset of Fig. 9 exhibits the variation of relative emission intensity with the incorporation of Gd^{3+}. When $x = 0.25$, the emission intensity arrives at its maximum value; the strongest emission peak located at 626 nm leads to the expected colorimetric purity.

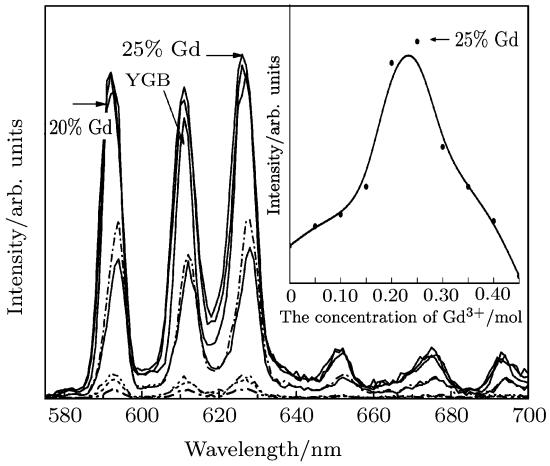


Fig. 9. Emission spectra of $Y_{0.75-x}Gd_xAl_{0.10}BO_3$: $Eu^{3+}_{0.10}$, $Bi^{3+}_{0.05}$ ($0.00 \leq x \leq 0.45$), with inset showing the concentration dependence of the relative integrated emission intensity of the sample ($\lambda_{ex} = 147$ nm).

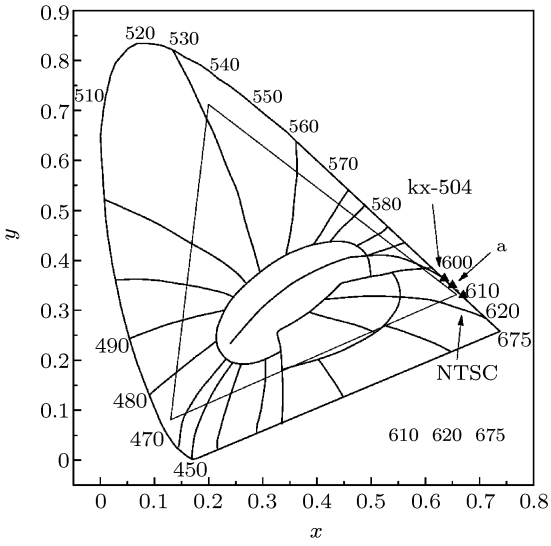


Fig. 10. Chromaticity coordinates of red commercial phosphor (YGB) and (a) $Y_{0.50}Gd_{0.25}Al_{0.10}BO_3:Eu^{3+}_{0.10}$, $Bi^{3+}_{0.05}$.

Figure 10 indicates the chromaticity coordinates of this sample (0.650, 0.350), which are closer to the NTSC (National Television Systems Committee) value of red phosphors (0.670, 0.330). Compared with the red commercial phosphor (Y, Gd) BO_3 (kx-504A), this sample has good chromaticity.

In a word, all results confirm that the sample $Y_{0.50}Gd_{0.25}Al_{0.10}BO_3:Eu^{3+}_{0.10}$, $Bi^{3+}_{0.05}$ possesses the appearance of a better spectral red and satisfactory luminous intensity. However, the content of Bi^{3+}, Gd^{3+} and Eu^{3+} must be optimized renewedly to achieve optimal luminescence.

When the concentrations above cause the samples to reach their maximum intensities, the intensity of the red emission decreases. These results show that the sensitization effect of the Gd^{3+} ion on Eu^{3+} emission varies with increasing Gd^{3+} concentration. Because of a higher concentration of Gd^{3+}, Gd^{3+}_n ion aggregates could form. These aggregates act as trapping centres and dissipate the absorbed energy through the nonradiative path, instead of the path of transferring energy to the activator Eu^{3+} ions.[24]

4. Conclusions

The single phase systems of $Y_{0.75-x}Gd_xAl_{0.10}BO_3:Eu^{3+}_{0.10}$, $0.05R^{3+}$ (R=Sc, Bi) ($0.00 \leq x \leq 0.45$) are synthesized and their luminescence properties are evaluated under excitations at 254 nm and 147 nm respectively. These results indicate that the charge transfer bands of all samples $O^{2-} \rightarrow Eu^{3+}$ are enhanced by substituting Y^{3+} with Bi^{3+}, Sc^{3+} and Gd^{3+} in both the UV and the VUV regions. Gd^{3+} and Bi^{3+} act as an intermediate "bridge" between the sensitizer and the activator Eu^{3+} in energy transfer to produce light in the (Y, Gd)BO_3:Bi^{3+}, Eu^{3+} system. The sample with the highest luminescent intensity can be obtained in the VUV region when 5% Sc^{3+} and 20% Gd^{3+}, or 5% Bi^{3+} and 25% Gd^{3+} are introduced into the (Y, Al)BO_3:Eu. Not only is the luminescence intensity of our sample superior to that of the red commercial phosphor (Y, Gd)BO_3:Eu, but its chromaticity is also better than that of the red commercial phosphor (Y, Gd) BO_3:Eu. This indicates that the improved red phosphor can be widely used as a PDP red phosphor.

References

[1] Luo W X, Huang S H, You F T and Peng H S 2007 *Acta Phys. Sin.* **56** 1765 (in Chinese)

[2] Wang Y H, Uheda K, Takizawa H, Mizumoto U and Endo T 2001 *J. Electrochem. Soc.* **148** G430

[3] Yang X L, Shi C S and Xu X L 2002 *Acta Phys. Sin.* **51** 2871 (in Chinese)

[4] Liu H Q, Wang L L and Qin W P 2004 *Acta Phys. Sin.* **53** 282 (in Chinese)
[5] Wang Y H, Endo T, He L and Wu C F 2004 *J. Cryst. Growth* **268** 568
[6] Wang L and Wang Y 2007 *J. Mater. Sci.* **43** 2908
[7] Hao Z and Blasse G 1985 *Mater. Chem. Phys.* **12** 257
[8] Gao C, Chen L, Bao J, Fu Y and Zhang G 2007 *J. Electrochem. Soc.* **154** J345
[9] Blasse G and Bril A 1967 *J. Chem. Phys.* **47** 5139
[10] Wang L L and Wang Y H 2007 *J. Lumin.* **122–123** 921
[11] Wang Y H, Guo X, Endo T, Murakami Y and Shirozawa M U 2004 *J. Solid State Chem.* **117** 2242
[12] Kingery W D, Bowen H K and Uhlmann D R 1976 *Introduction to Ceramics* 2nd ed. (New York: John Wiley and Sons)
[13] Park W, Summers J, Do Y R and Yang H G 2002 *J. Mater. Sci.* **37** 4041
[14] Zeng X, Im S J, Jang S H, Kim Y M, Park H B, Son S H, Hatanaka H, Kim G Y and Kim S G 2006 *J. Lumin.* **119–120** 121
[15] Veenis A W and Bril A 1978 *Philips J. Res.* **33** 124
[16] Kim C H, Bae H S, Pyun C H and Hong G Y 1998 *J. Korean Chem. Soc.* **42** 588
[17] Lai H, Yang H, Tao C Y and Yang X W 2007 *Phys. Stat. Sol.* (a) **204** 1178
[18] Kim C H, Park H L and Mho S 1997 *Solid State Commun.* **101** 109
[19] Wegh R T, Donker H, Oskam K D and Meijerink A 1999 *Science* **283** 663
[20] Zhang X, Zhang J, Liang L and Su Q 2005 *Mater. Res. Bull.* **40** 281
[21] Yang H C, Li C Y, He H, Tao Y, Xu J H and Su Q 2006 *J. Lumin.* **118** 61
[22] Zhang G L, Ba J F and Chen W J 1997 *Acta Phys. Sin.* **46** 177 (in Chinese)
[23] Chen L, Jiang Y, Chen S F, Zhang G B and Wang C 2008 *J. Lumin.* **128** 2048
[24] Leskeld M, Saakes M and Blasse G 1984 *Mater. Res. Bull.* **19** 151